JOURNAL OF AGRICULTURAL AND FOOD CHEMISTRY

Hydrogen Peroxide Induced Oxidative Stress Damage and Antioxidant Enzyme Response in Caco-2 Human Colon Cells

SUBHASHINEE S. K. WIJERATNE, SUSAN L. CUPPETT,* AND VICKY SCHLEGEL

Department of Food Science and Technology, University of Nebraska—Lincoln, Lincoln, Nebraska 68583-0919

Studies were conducted to evaluate the cell damage caused by exposing human colon carcinoma cells, Caco-2, to hydrogen peroxide at concentrations varying from 0 to 250 μM for 30 min. Evaluation of cell viability, as measured by trypan blue dye exclusion test, showed that the loss of viability was <5% at concentrations up to 250 μM hydrogen peroxide. Cell membrane damage and DNA damage as measured by the leakage of lactate dehydrogenase and the comet assay, respectively, were significantly high at concentrations >100 μM hydrogen peroxide compared to those of the control. Antioxidant mechanisms in Caco-2 cells were evaluated by measuring catalase, superoxide dismutase, and glutathione peroxidase activities. Catalase activities remained constant in cells treated with 50−250 μM hydrogen peroxide. Superoxide dismutase activity decreased, whereas glutathione peroxidase activity increased in cells treated with H_2O_2 concentrations of >50 μM. This study showed that with increasing hydrogen peroxide concentration, cell membrane leakage and DNA damage increased, whereas the three antioxidant enzymes responded differently, as shown by mathematical models.

KEYWORDS: Caco-2; colon; oxidative stress; hydrogen peroxide; antioxidant enzymes; catalase; superoxide dismutase; glutathione peroxidase; DNA damage; cell viability

INTRODUCTION

Oxidative stress occurs when the production of oxidizing agents, free radicals and reactive oxygen species (ROS), exceeds the antioxidant capacity of cellular antioxidants in a biological system. This imbalance between oxidants and antioxidants leads to tissue injuries and to the progression of degenerative diseases in humans, such as coronary heart disease (*1*), cataracts (*2*), muscle degeneration (*3*), aging (*4*), and cancer (*5*, *6*). The American Cancer Society estimated in 2005 that >0.5 million Americans will die from cancer. Approximately 56300 of these deaths will be caused by colorectal cancer, the second major cause of cancer deaths in the United States. In addition, 12000 will die due to stomach and small intestinal cancers (*7*). Oxidative stress contributes to cancer development through increasing cell proliferation and survival, increasing cellular migration, and inducing DNA damage that leads to genetic lesions (*5*). Oxidative stress also leads to the development of other intestinal pathological conditions such as inflammatory bowel disease and ischemic-reperfusion injury (*8*). Therefore, it is important to study the damaging effects of oxidative stress on the intestinal epithelium and to understand protective mechanisms by which the cells respond to stress. Cell membranes protect the integrity of cells by selectively regulating cell permeability. Oxidative degradation of membrane lipids can result in loss of membrane integrity, defective membrane transport mechanisms, and increased permeability; thus, lesser injury causes minor cell damage, whereas major injury leads to cell death.

Table 1. Detoxification Activities of Antioxidant Enzymes in Vivo

enzyme	activity
superoxide dismutase	dismutation of superoxide to H_2O_2
glutathione peroxidase (cellular)	decomposition of H_2O_2 and free acid hydroperoxide
glutathione peroxidase (plasma)	decomposition of H_2O_2 and phospholipid hydroperoxide
phospholipid hydroperoxide glutathione peroxidase	decomposition of phospholipid hydroperoxide
catalase	decomposition of H_2O_2
glutathione-*S*-transferase	decomposition of lipid hydroperoxide

Mammalian cells possess inherent antioxidant mechanisms to scavenge and/or neutralize ROS. These mechanisms are mainly due to antioxidant enzymes that are presented in **Table 1**. Of these enzymes, superoxide dismutase (SOD), catalase, and glutathione peroxidase (GPx) are considered to be the most important (*9*). However, there is a lack of information on how the activities of these enzymes differ in oxidatively stressed intestinal cells compared to nonstressed cells.

The Caco-2 cell line has been widely used as an in vitro model for the small intestine; the Caco-2 monolayer exhibits features such as brush border microvilli, tight junctions, and dome formation, which are characteristic of the intestinal epithelium (*10*). In conjunction with oxidative stress studies

* Corresponding author [telephone (402) 472 5616; fax (402) 472 1693; e-mail slcuppet@unlnotes.unl.edu].

10.1021/jf0512003 CCC: $30.25
Published on Web 10/01/2005

these cells have also been effectively used as an in vitro model for many applications such as screening drugs for their intestinal absorption potential (*11*), investigation of toxicants, food mutagens, and their mechanisms (*12*, *13*), and studying the absorption of minerals and phenolics (*14*−*16*). It has been observed that Caco-2 cells exhibit small but significantly different antioxidant enzyme profiles with increasing time of culturing (*9*). Therefore, for studies conducted to compare the changes in enzymes at different stress levels, it is important to maintain constant culture conditions throughout the study and utilize cells on a predetermined day of culturing.

This paper presents the effects of oxidative damage and changes in antioxidant enzymes in Caco-2 cells, induced by hydrogen peroxide at various concentrations. Oxidative stress-related cellular damage was investigated by assessing cell viability, membrane integrity, lipid oxidation, and DNA damage. Changes in antioxidant enzymes were evaluated by quantifying activities of catalase, SOD, and GPx.

MATERIALS AND METHODS

Materials. A human colon carcinoma cell line (Caco-2) was obtained from the American Type Culture Collection (Rockville, MD). Dulbecco's Modified Eagle Medium (DMEM) and fetal bovine serum (FBS) were purchased from Invitrogen Corp. (Carlsbad, CA). L-Glutamine, penicillin with streptomycin, trypsin with ethylenediaminetetraacetic acid (EDTA), and phosphate-buffered saline (PBS) were purchased from Fisher Scientific (Fair Lawn, NJ). Trypan blue, nonessential amino acid solution, xanthine, hypoxanthine, nitro blue tetrazolium, diethylenetriaminepentaacetic acid, lactate dehydrogenase (LDH) based TOX-7 kit, and glutathione peroxidase cellular activity assay kit CGP-1 were obtained from Sigma Chemicals (St. Louis, MO). Hydrogen peroxide, chloroform, cyclohexane, and ethanol were purchased from VWR International (Bridgeport, NJ). Micro BCA protein assay kit was purchased from Pierce Biotechnology (Rockford, IL).

Methods. *Culture and Oxidation of Caco-2 Cells.* Caco-2 cells were grown in DMEM supplemented with 20% FBS, 1% L-glutamine, 1% nonessential amino acids, and 50 μg/mL penicillin with streptomycin. The cell cultures were maintained at 37 °C in a humidified atmosphere with 5% CO_2 and were seeded onto collagen-coated 25 or 75 cm^2 area culture flasks. Cells were harvested by a brief (6 min) trypsinization and then centrifuged (Beckman GS-15R centrifuge, Beckman, Palo Alto, CA) at 200*g* for 5 min. Oxidation was induced by exposing Caco-2 cells to 0−250 μM hydrogen peroxide (H_2O_2) in FBS-free DMEM or PBS, supplemented with 1% L-glutamine and 1% nonessential amino acids, for 30 min on the fourth day of culturing after reaching confluency. This time−concentration combination was chosen as the oxidative treatment because the intention of this study was to determine the cellular responses at stressed conditions without inducing cell death. Preliminary studies indicated that incubating Caco-2 cells with H_2O_2 concentrations >500 μM, for a period of 1 h or more, caused cell death or cell detachment from culture flasks.

Cell Viability. Cell viability was assessed using the trypan blue dye exclusion method (*17*). A suspension of $\sim 10^6$ cells/mL was prepared using brief trypsinization of treated and untreated cells. One hundred microliters of the cell suspension was mixed with 100 μL of trypan blue and left for 5 min at room temperature. Approximately 20 μL of this mixture was transferred using a micropipet to the counting chamber of a Neubauer hemocytometer (VWR Scientifics, West Chester, PA). The stained (dead) cells and the total cells per square of a Neubauer cell chamber (three squares per suspension) were counted after the Neubauer hemocytometer had been placed under a microscope (Microscoptics IV900 series, VWR Scientifics). Depending on the cell titers, generally 50−150 cells were visible in each square.

Cell Membrane Damage. Cells were grown to confluence in 25 cm^2 culture flasks and washed with PBS prior to use. Different concentrations of H_2O_2 (0−250 μM) in PBS supplemented with 1% L-glutamine and 1% nonessential amino acids were used to induce oxidation. After 30 min of exposure, PBS from each flask was collected. Damage to plasma membrane by hydrogen peroxide was studied by measuring the release of lactic acid dehydrogenase (LDH) from injured cells. LDH leakage into PBS and total LDH activity (LDH leakage to PBS plus LDH in remaining cells) were measured with an in vitro cytotoxicity assay kit, lactate dehydrogenase based TOX-7 (Sigma Chemicals), and corrected by the activity already present in the medium of untreated cells. The assay is based on the reduction of NAD to NADH by LDH. NADH is utilized to convert a tetrazolium dye in the assay kit to a colored compound with an absorption maximum at 490 nm. The intensity of the color is indicative of LDH activity in the assay medium, and the LDH activity was measured spectrophotometrically (Beckman Coulter DU800 spectrophotometer, Beckman Coulter Inc., Fullerton, CA) at 490 nm. LDH activity in the PBS supernatant was determined as a percentage of the total LDH activity.

Preparation of Cell Lysates. Culture medium was decanted, and cells were washed with 5−10 mL of PBS. The cells were harvested by a brief trypsinization. Cell suspensions were centrifuged at 200*g* for 5 min and washed twice with 5 mL of PBS. Supernatants were discarded and cell pellets resuspended in 5 mL of PBS at 0 °C and then placed on ice. Cells were lysed using a mini-bead beater (Biospec Products, Bartlesvillle, OK) for 10 s at 4200 rpm. The lysates were centrifuged (Beckman GS-15R centrifuge) at 14000*g* for 10 min at 4 °C and supernatants immediately used for lipid peroxidation and antioxidant enzyme assays.

Lipid Peroxidation Assay. Lipid peroxidation was assayed by measuring conjugated dienes in cell lysates. Conjugated dienes were quantified according to the method described by Buege and Aust (*18*). One milliliter of cell lysate in PBS was mixed thoroughly with 5 mL of chloroform/methanol (2:1) solution, followed by centrifugation (Beckman GS-15R centrifuge) at 1000*g* for 5 min until phase separation. Most of the upper layer was removed by suction, and 3 mL of the lower chloroform layer was transferred to a test tube. The chloroform layer was removed under nitrogen infusion, and the lipid residue was dissolved in 1.5 mL of cyclohexane. The absorbance of the solution at 233 nm was measured (Beckman Coulter DU800 spectrophotometer) against a cyclohexane blank at 233 nm. Conjugated dienes were reported as the optical density units at 233 nm.

Antioxidant Enzyme Activity. A modified version of the Nishikimi et al. (*19*) method was used to detect superoxide dismutase activity in cell lysates. Superoxide radicals were generated using a xanthine oxidase/hypoxanthine system. The reaction mixture contained 1 mL of 3 mM hypoxanthine, 1 mL of 100 mIU xanthine oxidase, 1 mL of 12 mM diethylenetriaminepentaacetic acid, 1 mL of 178 μM nitro blue tetrazolium, and 1 mL of the cell lysate. All solutions were prepared in PBS. The absorbance of the mixtures at 560 nm was recorded initially at 0 min and thereafter at 5 min intervals up to 30 min. Superoxide radical-scavenging capacities (percent) of the cell lysates at the end of 30 min were calculated with the equation $[1 - (A/B)] \times 100$, where A = absorbance of the medium containing cell lysate at 30 min and B = absorbance of the medium without cell lysate at 30 min (blank). Catalase was assayed spectrophotometrically at 25 °C by following the extinction of H_2O_2 at 240 nm (*20*). The catalase activity per milliliter of the cell lysate was calculated as the reduction of H_2O_2 mmol L^{-1} min^{-1} mL^{-1}. Nonenzymatic H_2O_2 decomposition (baseline) was subtracted from each determination. The cell glutathione peroxidase (GPx) activity was measured using the GPx cellular activity assay kit CGP-1 (Sigma Chemicals). This kit uses an indirect method, based on the oxidation of glutathione (GSH) to oxidized glutathione (GSSG) catalyzed by GPx, which is then coupled with recycling GSSG back to GSH utilizing glutathione reductase (GR) and NADPH. The decrease in NADPH at 340 nm during oxidation of NADPH to NADP is indicative of GPx activity. The activity of GPx per milliliter of the cell lysate was calculated as the decrease in NADPH μmol min^{-1} mL^{-1}.

DNA Damage by Comet Assay. The comet assay was performed using Trevigen's comet assay reagent kit for single-cell electrophoresis assay (Trevigen Inc., Gaithersberg, MD). Cells (1×10^5) were suspended in 1 mL of ice-cold PBS. Fifty microliters of the cell suspension was combined with 500 μL of prewarmed low melting point (LMP) agarose, and 75 μL of this mixture was immediately pipetted onto a CometSlide. Slides were placed flat at 4 °C in the dark for 30

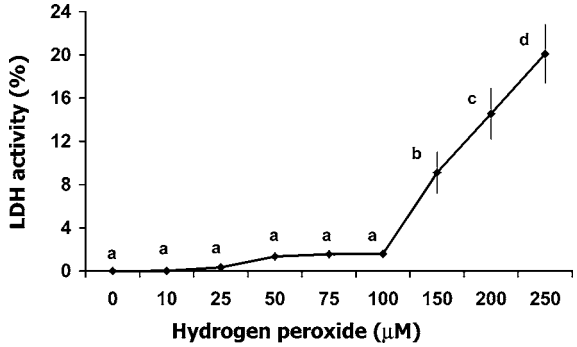

Figure 1. Lactic acid dehydrogenase activity in the assay medium as a percentage of total cell LDH activity. Caco-2 cell cultures were incubated with different concentrations of H_2O_2 (0, 10, 25, 50, 75, 100, 200, 250 μM). Each point represents the mean ± SD of four determinations. Different letters indicate significantly different observations ($p < 0.05$).

min for gelling. After completion of gelling, slides were transferred to a prechilled lysis solution (2.5 M sodium chloride, 100 mM EDTA, pH 10, 10 mM Tris base, 1% sodium lauryl sarcosinate, and 1% Triton X-100) and placed at 4 °C for 50 min. Slides were then incubated in a fresh electrophoresis buffer (0.3 M NaOH, 1 mM EDTA, pH 13) for 40 min at room temperature to allow unwinding of DNA. Electrophoresis was carried out at room temperature in fresh electrophoresis buffer for 40 min at 1 V/cm and 300 mA. After electrophoresis, slides were gently rinsed by dipping several times in distilled water and then immersed in 70% ethanol for 5 min and air-dried. Slides were stored with desiccant at room temperature prior to analysis. Slides were stained with SYBR green and viewed by an Olympus AX70TRF microscope digital camera system (Olympus Optical Co. Ltd.). Digital images of DNA were analyzed using NIH Image software available at http://rsb.info.nih.gov/ij/. About 100−150 cells were scored per sample.

Statistical Design. A randomized complete block design was used in all test systems. All experiments were repeated at least four times. Statistical analysis was conducted using Statistical Analysis System (SAS) software (SAS Institute Inc., Cary, NC) with one-way analysis of variance (ANOVA) followed by Tukey's HSD test for significant differences and to fit suitable models to explain antioxidant enzyme activity. Unless stated otherwise, a p value of ≤ 0.05 was considered to be statistically significant.

RESULTS

Cell Damage. LDH release to culture medium (**Figure 1**) was very low (<2%) in Caco-2 cells treated with 0−100 μM H_2O_2. A significant increase in LDH leakage, compared to control cells (0 μM H_2O_2), was detected in cells subjected to 150 μM H_2O_2 and further increased to 20% at 250 μM H_2O_2. However, cells maintained 95% viability, indicated by trypan blue dye exclusion test, when treated with 0−250 μM H_2O_2 concentrations (data not shown). Conjugated dienes were between 0.05 and 0.07 optical density units (data not shown), which indicated there was no or very little cellular lipid peroxidation in cells treated with 0−250 μM H_2O_2.

DNA Damage. DNA damage of cells treated with 50−100 μM H_2O_2 was not significantly different from that of the control cells (**Figure 2**). At higher concentrations, DNA damage increased continuously with increasing H_2O_2 concentration.

Antioxidant Enzyme Activity. Catalase, SOD, and GPx enzyme activities at different H_2O_2 concentrations are presented in **Table 2**. Catalase activity was significantly higher than that of the control in all cells treated with H_2O_2 up to 250 μM. There was no significant difference in catalase activity in cells treated with 50−250 μM H_2O_2. SOD activity was highest in cells treated with 50 μM H_2O_2, and then its activity gradually

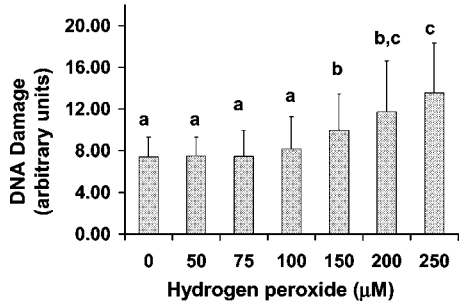

Figure 2. DNA damage in Caco-2 cells as measured by comet assay. Caco-2 cell cultures were incubated with different concentrations of H_2O_2 (0, 50, 75, 100, 200, 250 μM). Each point represents the mean ± SD of four determinations. Different letters indicate significantly different observations ($p < 0.05$).

Table 2. Antioxidant Enzyme Activity[a] in Caco-2 Cells Treated with Hydrogen Peroxide

H_2O_2 concn used to treat cells (μM)	catalase activity[b]	SOD activity[c]	GPx activity[d]
0	0.534 ± 0.004 a	28.8 ± 2.1 cd	0.31 ± 0.05 a
50	0.991 ± 0.033 b	36.2 ± 3.1 e	0.31 ± 0.04 a
75	0.983 ± 0.033 b	30.8 ± 1.5 d	0.31 ± 0.03 a
100	0.966 ± 0.017 b	26.5 ± 1.2 d	0.40 ± 0.03 ab
150	0.966 ± 0.014 b	18.5 ± 1.1 b	0.50 ± 0.03 bc
200	0.966 ± 0.012 b	15.2 ± 1.1 ab	0.55 ± 0.04 c
250	0.967 ± 0.011 b	13.2 ± 1.1 a	0.60 ± 0.05 c

[a] Results are mean values of four determinations ± standard deviation. Means within a column having different letters are significantly ($p < 0.05$) different from one another. [b] Decrease in H_2O_2 mmol L^{-1} min^{-1} mL^{-1}. [c] Superoxide radical scavenged (%). [d] Decrease in NADPH μmol L^{-1} min^{-1} mL^{-1}.

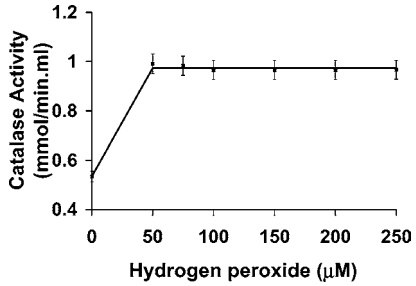

Figure 3. Catalase activity (decrease in H_2O_2 mmol L^{-1} min^{-1} mL^{-1}) in Caco-2 cells as depicted by the monomolecular regression model. Caco-2 cell cultures were incubated with different concentrations of H_2O_2 (0, 50, 75, 100, 200, 250 μM). Each point represents the mean ± SD of four determinations.

decreased with increasing H_2O_2 concentrations. However, SOD activities at 75 and 100 μM H_2O_2 concentrations were not significantly different from that of the control. In contrast, GPx activity of cells increased significantly beyond 100 μM H_2O_2 and continued to increase, reaching a maximum at 250 μM H_2O_2. GPx activity of cells treated with 50, 75, and 100 μM H_2O_2 was not significantly different from that of the control.

Nonlinear regression was used to predict suitable models that would depict the differences in the activities of these enzymes in Caco-2 cells treated with 0−250 μM H_2O_2. It was observed that catalase (**Figure 3**) activity could be explained using a monomolecular regression model [$Y = \alpha - (\beta \times \exp(-\kappa X)$], whereas SOD activity (**Figure 4**) followed a third-order polynomial response curve. A better fit for GPx activity (**Figure**

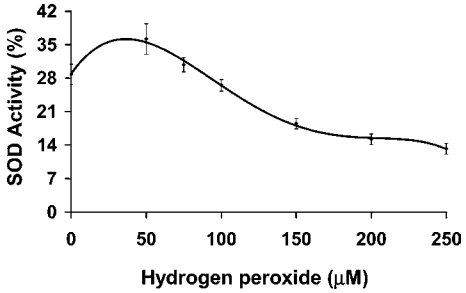

Figure 4. Superoxide dismutase activity (percent of scavenged superoxide radicals) in Caco-2 cells as depicted by the third-order polynomial model. Caco-2 cell cultures were incubated with different concentrations of H_2O_2 (0, 50, 75, 100, 200, 250 μM). Each point represents the mean ± SD of four determinations.

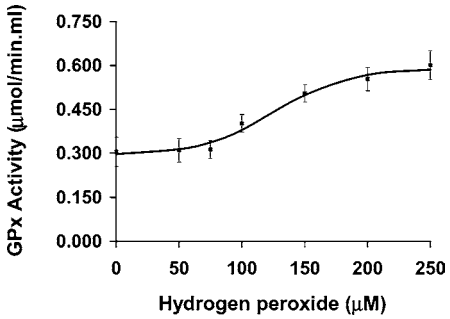

Figure 5. Glutathione peroxidase activity (decrease in NADPH μmol L^{-1} min^{-1} mL^{-1}) in Caco-2 cells as depicted by the inflection point logistic model. Caco-2 cell cultures were incubated with different concentrations of H_2O_2 (0, 50, 75, 100, 200, 250 μM). Each point represents the mean ± SD of four determinations.

5) was an inflection point logistic model [$Y = \delta + (\alpha - \delta)/(1 + \exp(-\kappa(X - \tau)))$]. The model equations, and their corresponding regression coefficient (R^2) or pseudo R^2 values (*21*), for the activities of enzymes, catalase (Y_{CAT}), SOD (Y_{SOD}), and GPx (Y_{GPx}), are given below.

$$Y_{CAT} = 0.9732 - (0.4392 \times \exp(-0.5259X)$$

$$(\text{psuedo } R^2 = 0.9963)$$

$$Y_{SOD} = -7E{-}08X^4 + 4E{-}05X^3 - 0.0084^2 + 0.4508X + 28.893$$

$$(R^2 = 0.9965)$$

$$Y_{GPx} = 0.3 + (0.5902 - 0.2933)/(1 + \exp((-0.0341)(X - 126.3))$$

$$(\text{psuedo } R^2 = 0.9797)$$

X = hydrogen peroxide concentrations from 0 to 250 μM, Y_{CAT} = reduction of H_2O_2 mmol L^{-1} min^{-1} mL^{-1}, Y_{SOD} = percentage of scavenged superoxide radicals, and Y_{GPx} = consumption of NADPH μmol L^{-1} min^{-1} mL^{-1}.

These curves show that maximum activities of the three antioxidant enzymes occur at different concentrations of H_2O_2. Cellular catalase reached a maximum activity at 50 μM H_2O_2 and remained constant throughout treatments up to 250 μM H_2O_2, whereas SOD showed a maximum activity at 35 μM H_2O_2. For GPx activity, the model shows a maximum activity (α) at 250 μM H_2O_2 and an occurrence of maximum rate of activity at 126 μM H_2O_2. In other words, the inflection point (τ), the H_2O_2 concentration at which the rate of GPx activity started to decrease, is 126 μM H_2O_2. The intrinsic relative rate (κ), that is, GPx activity when the effects of limiting factors are negligible, is 0.034. The polynomial response curve for SOD also showed a shift in enzyme activity near 100 μM H_2O_2, rendering it a critical concentration in terms of antioxidant enzyme capabilities. Catalase activity, as explained by a monomolecular model, shows that its activity is limited at a reduction of 0.9732 H_2O_2 mmol L^{-1} min^{-1} mL^{-1}. The activity is bound at this level and could be due to many factors that should be further investigated.

DISCUSSION

Hydrogen peroxide present in aerobic cells as a metabolite in low concentrations is generated by nonenzymatic and superoxide dismutase-catalyzed dismutation reactions (*22*). The biologically significant reaction of H_2O_2 is its spontaneous conversion, catalyzed by Fe^{2+} (Fenton reaction), to the highly reactive hydroxyl radicals ($HO^{\bullet}$) that react instantaneously with any biological molecule from which it can abstract a hydrogen atom (*23*). As ingested foods frequently contain iron salts, and reducing agents in gastric juice reduce iron to Fe^{2+} to facilitate its absorption, the gastrointestinal (GI) tract is a major target for damage by hydroxyl radicals generated by Fenton reaction (*24*, *25*). Several studies have also shown the involvement of H_2O_2 in the progression of colon cancer (*25*−*27*).

H_2O_2 at higher concentrations (>100 μM) causes cell membrane damage to Caco-2 cells as detected by increased lactate dehydrogenase leakage, which indicates a change in membrane permeability or cell necrosis. A change in membrane permeability disturbs the structural integrity, which could lead to the increased entry of toxins to cells, which eventually results in cell death at a later stage. The changes in permeability of Caco-2 cells exposed to H_2O_2 have been attributed to disruption of paracellular junctional complexes resulting from tyrosine phosphorylation of membrane proteins (*28*, *29*). However, in this study there was no indication of a loss of cell viability or cell lipid peroxidation in cells treated for 30 min with 0−250 μM H_2O_2. When Caco-2 cells were treated with ≥250 μM H_2O_2 for 90 min, a 3-fold increase in lipid peroxidation compared to control cells was observed as measured by thiobarbituric acid reactive substances (TBARS) (*30*). Higher doses of H_2O_2 (10 mM) on Caco-2 cells caused a decrease in cell viability and also caused an increase in intracellular malondialdehyde content, indicating the occurrence of lipid peroxidation (*31*). Similar results (*31*) were shown when cells were treated with 100 μM H_2O_2 for 2 h (*32*). These results indicate that the effects of H_2O_2 on Caco-2 cells are both time and concentration dependent.

The comet assay, also known as single-cell gel electrophoresis (SCG), is an electrophoresis technique used to detect DNA damage in individual cells. Damage is represented by an increase of DNA fragments that have migrated out of the cell nucleus in the form of a characteristic streak similar to the tail of a comet (*33*). The DNA fragments are generated by DNA double-strand breaks, single-strand breaks, and/or strand breaks induced by alkali-labile sites. In the alkaline version of the assay DNA damage can be assessed using different parameters, such as the tail length, relative tail fluorescent intensity, and tail moment (*33*, *34*). Results of this study showed DNA damage at 150−250 μM H_2O_2, and it is known that DNA damage in Caco-2 cells by H_2O_2 at concentrations of <300 μM H_2O_2 is dominated by single-strand breaks (*35*). Unlike double-strand breaks, a

single-strand break in DNA is quickly repaired through simple reinsertion of the complementary base using an unbroken strand as a template. Properly repaired DNA will restore cells to their normal state, whereas incorrect DNA repair will result in mutations in DNA (*36*, *37*). Also, if damaged DNA replicates before it is repaired, a permanent DNA alteration could occur, again leading to carcinogenesis. Therefore, cells with rapid turnover rates, such as intestinal epithelial cells, are more susceptible to malignant transformations (*38*, *39*).

The susceptibility of a tissue to oxidative injuries depends mainly on their antioxidant defense mechanisms. Lack of antioxidant enzymes makes a tissue more susceptible to oxidative damages. The antioxidant enzyme activity of cells is determined by inherent characteristics of the cells, their metabolic specialization, and environmental factors to which the cells are exposed such as the level of oxygenation and the presence of metabolites (*40*). As an example, the liver possesses and maintains massive antioxidant machinery because it handles oxidative metabolism of a variety of substrates, whereas the colon, which does not engage extensively in such metabolic processes, contains lower amounts of antioxidants (*41*). The distribution of antioxidants within colonic tissue also varies depending on what part of the tissue is more prone to oxidative damage. Early investigators have shown that antioxidant enzymes in colonic epithelial cells exhibit higher activity compared to that of its mucosa (*40*, *41*). Even with adequate oxidant defense mechanisms, tissues such as gastrointestinal epithelium can be overwhelmed by fluxes of oxidants. Therefore, understanding tissue-mediated defense mechanisms and tolerance levels of enzymes to oxidative damage becomes more important in deciding effective strategies to prevent or reduce cellular oxidative damage.

Superoxide dismutase, catalase, and glutathione peroxidase are considered to be the most important enzymes in protecting oxidatively challenged tissues. Catalase, a porphyrin-containing enzyme, converts hydrogen peroxide to water and oxygen (*42*), and most of it is located in peroxisomes (*43*). Superoxide dismutase converts superoxide anion to hydrogen peroxide (*44*). In animal cells, Cu/Zn SOD is present both in cytosol and in mitochondria, whereas Mn-SOD is present only in mitochondria. Glutathione peroxidase is responsible for the removal of hydrogen peroxide and other organic hydroperoxides (*45*) and is abundant in cytosolic and mitochondrial compartments. Catalase and SOD do not consume cofactors because they are dismutases, but selenium-dependent GPX, which is a peroxidase, requires NADPH to regenerate its reducing coenzyme (*46*).

In this study, GPx activity was elevated with increasing H_2O_2 concentrations, whereas catalase activity remained constant at all tested H_2O_2 treatments, indicating that GPx was more active than catalase in removing H_2O_2. Even in cells such as erythrocytes where catalase contents are very high, H_2O_2 is degraded by glutathione peroxidase (*47*). This is consistent with the very high K_m of catalase that is close to 1 M (*43*). SOD is inhibited by H_2O_2 in a dose- and time-dependent manner (*48*, *49*), and our study revealed that SOD activity in Caco-2 cells was negatively affected by H_2O_2 at concentrations starting around 35 μM and became severe above 100 μM. These results agree with those of Liu and others (*32*), who found a significant decrease in cell survival and SOD activity in intestinal epithelial cells treated with 100 μM H_2O_2 for 2 h. In contrast, pure SOD in a noncellular system showed increased oxidation−reduction capacity when exposed to 250−1000 μM H_2O_2 for 15 min. However, SOD activity decreased dramatically with longer exposure durations to H_2O_2 (*50*). In our study, Caco-2 cells still showed some SOD activity at 250 μM H_2O_2, suggesting that total inhibition of SOD was not attained during the 30 min of oxidative treatment. Inhibition of SOD by H_2O_2 could be associated with the reduction of the active site (Cu^{2+}) in SOD to Cu^{+} (*49*), the destruction of histidine that is close to Cu^{2+} (*48*), and/or the structure alteration of SOD that restricts access to Cu^{2+} (*50*).

Antioxidant enzymes exhibit synergistic interactions by protecting each other from specific free radical attacks (*48*, *51*, *52*). SOD protects catalase and GPx from inactivation by superoxide radicals (*51*), whereas catalase and GPx protect SOD from inactivation by hydroperoxides (*48*, *52*). The protective effects by catalase and GPx may have been responsible for the activity of SOD that was present in cells treated with higher H_2O_2 concentrations. However, there could be other factors that play a role in oxidative stress related enzymatic activities. In a biological system the observed effect of an enzyme would thus be the net effect all synergistic and antagonistic effects of other enzymes and compounds present in the cellular environment.

In summary, this study showed that cells were able to maintain their viability at 0−250 μM H_2O_2, which could be attributed to efficient antioxidant mechanisms, mediated by catalase, GPx, and SOD present in the colon cells. Results showed that 50−250 μM H_2O_2 concentrations increased GPx activity and decreased SOD activity but did not change catalase activity in Caco-2 cells. This is the first study in which mathematical models were applied to describe differences in antioxidant enzyme activities due to stress induced by various concentrations of H_2O_2. Using a high dose of H_2O_2 (>100 μM) on Caco-2 cells caused changes in membrane integrity and significant DNA damage. This indicates that colon cells are susceptible to oxidative activity of H_2O_2, emphasizing the fact that the Caco-2 cell model is indeed an ideal system to conduct studies related to oxidation stress. Future studies are directed toward identifying antioxidants that can eliminate or reduce oxidative stress in colon cells.

LITERATURE CITED

(1) Stocker, R.; Keaney, J. F., Jr. Role of oxidative modifications in atherosclerosis. *Physiol. Rev.* **2004**, *84*, 1381−1478.

(2) Shichi, H. Cataract formation and prevention. *Expert Opin. Invest. Drugs* **2004**, *13*, 691−701.

(3) Caporossi, D.; Ciafre, S. A.; Pittaluga, M.; Savini, I.; Farace, M. G. Cellular responses to H_2O_2 and bleomycin-induced oxidative stress in L6C5 rat myoblasts. *Free Radical Biol. Med.* **2003**, *35*, 1355−1364.

(4) Ben-Porath, I.; Weinberg, R. A. The signals and pathways activating cellular senescence. *Int. J. Biochem. Cell. Biol.* **2005**, *37*, 961−976.

(5) Storz, P. Reactive oxygen species in tumor progression. *Front. Biosci.* **2005**, *10*, 1881−1896.

(6) Tandon, R.; Khanna, H. D.; Dorababu, M.; Goel, R. K. Oxidative stress and antioxidant status in peptic ulcer and gastric carcinoma. *Indian J. Physiol. Pharmacol.* **2004**, *48*, 115−118.

(7) Jemal, A.; Murray, T.; Ward, E.; Samuels, A.; Tiwari, R. C.; Ghafoor, A.; Feuer, E. J.; Thun, M. J. Cancer Statistics 2005. *Ca—Cancer J. Clin.* **2005**, *55*, 10−30.

(8) Thomson, A.; Hemphill, D.; Jeejeebhoy, K. N. Oxidative stress and antioxidants in intestinal disease. *Dig. Dis.* **1998**, *16*, 152−158.

(9) Baker, S. S.; Baker, R. D. Antioxidant enzymes in the differentiated Caco-2 cell line. *In Vitro Cell Dev. Biol.* **1992**, *28*, 643−647.

(10) Pinto, M.; Robine-Leon, S.; Appay, M.-D.; Kedinger, M.; Triadou, N.; Dussaulx, E.; Lacrox, B.; Simon-Assmann, P.; Haffen, K.; Fogh, J.; Zweibaum, A. Enterocyte-like differentiation and polarization of the human colon carcinoma cell line Caco-2 in culture. *Biol. Cell* **1983**, *47*, 323−330.

(11) Pal, D.; Udata, C.; Mitra, A. K. Transport of cosalane—a highly lipophilic novel anti-HIV agent—across Caco-2 cell monolayers. *J. Pharm. Sci.* **2000**, *89*, 826−833.

(12) Okada, T.; Narai, A.; Matsunaga, S.; Fusetani, N.; Shimizu, M. Assessment of the marine toxins by monitoring the integrity of human intestinal Caco-2 cell monolayers. *Toxicol. In Vitro* **2000**, *14*, 219−226.

(13) Walle, U. K.; Walle, T. Transport of the cooked-food mutagen 2-amino-1-methyl-6-phenylimidazo-[4,5-*b*]pyridine (PhIP) across the human intestinal Caco-2 cell monolayer: role of efflux pumps. *Carcinogenesis* **1999**, *20*, 2153−2157.

(14) Andreasen, M. F.; Kroon, P. A.; Williamson, G.; Garcia-Conesa, M.-T. Intestinal release and uptake of phenolic antioxidant diferulic acids. *Free Radical Biol. Med.* **2001**, *31*, 304−314.

(15) Vaidyanathan, J. B.; Walle, T. Transport and metabolism of the tea flavonoid (−)-epicatechin by the human intestinal cell line Caco-2. *Pharm. Res.* **2001**, *18*, 1420−1425.

(16) Glahn, R. P.; Wortley, G. M.; South, P. K.; Miller, D. D. J. Inhibition of iron uptake by phytic acid, tannic acid, and $ZnCl_2$: studies using an in vitro digestion/Caco-2 cell model. *J. Agric. Food Chem.* **2002**, *50*, 390−395.

(17) Pool-Zobel, B. L.; Lotzmann, N.; Knoll, M.; Kuchenmeister, F.; Lambertz, R.; Leucht, U.; Schroder, H. G.; Schmezer, P. Detection of genotoxic effects in human gastric and nasal mucosa cells isolated from biopsy samples. *Environ. Mol. Mutagen.* **1994**, *24*, 23−45.

(18) Buege, J. A.; Aust, S. D. Microsomal lipid peroxidation. *Methods Enzymol.* **1978**, *52*, 302−310.

(19) Nishikimi, M.; Rao, N. A.; Yagi, K. The occurrence of superoxide anion in the reaction of reduced phenazine methosulphate and molecular oxygen. *Biochem. Biophys. Res. Commun.* **1972**, *46*, 849−854.

(20) Beers, R. F.; Sizer, I. W. A spectrophotometric method for measuring the breakdown of hydrogen peroxide by catalase. *J. Biol. Chem.* **1952**, *195*, 133−140.

(21) Kvålseth, T. O. Cautionary note about R^2. *Am. Stat.* **1985**, *39*, 279−285.

(22) Kanner, J. Mechanism of nonenzymic lipid oxidation in muscle foods. In *Lipid Oxidation in Food*; St. Angelo, A. J., Ed.; American Chemical Society: Washington, DC, 1992; pp 55−73.

(23) Halliwell, B.; Gutteridge, J. M. C. *Free Radicals in Biology and Medicine*, 3rd ed.; Clarendon Press: Oxford, U.K., 1999; pp 36−104.

(24) Halliwell, B.; Zhao, K.; Whiteman, M. The gastrointestinal tract: a major site of antioxidant action? *Free Radical Res.* **2000**, *33*, 819−830.

(25) Glei, M.; Latunde-Dada, G. O.; Klinder, A.; Becker, T. W.; Hermann, U.; Voigt, K.; Pool-Zobel, B. L. Iron-overload induces oxidative DNA damage in the human colon carcinoma cell line HT29 clone 19A. *Mutat. Res.* **2002**, *519*, 151−161.

(26) Pool-Zobel, B. L.; Leucht, U. Induction of DNA damage by risk factors of colon cancer in human colon cells derived from biopsies. *Mutat. Res.* **1997**, *375*, 105−115.

(27) Zhu, J. W.; Yu, B. M.; Ji, Y. B.; Zheng, M. H.; Li, D. H. Upregulation of vascular endothelial growth factor by hydrogen peroxide in human colon cancer. *World J. Gastroenterol.* **2002**, *8*, 153−157.

(28) Rao, R.; Baker, R. D.; Baker, S. S. Inhibition of oxidant-induced barrier disruption and protein tyrosine phosphorylation in Caco-2 cell monolayers by epidermal growth factor. *Biochem. Pharmacol.* **1999**, *5*, 685−695.

(29) Rao, R. K.; Baker, R. D.; Baker, S. S.; Gupta, A.; Holycross, M. Oxidant-induced disruption on intestinal epithelial barrier function: role of protein tyrosine phosphorylation. *Am. J. Physiol.* **1997**, *273*, G812−G823.

(30) Martin, K. R.; Failla, M. L.; Smith, J. C., Jr. Differential susceptibility of Caco-2 and HepG2 human cell lines to oxidative stress. *J. Elisha Mitchell Sci. Soc.* **1997**, *113*, 149−162.

(31) Manna, C.; Galletti, P.; Cucciolla, V.; Moltedo, O.; Leone, A.; Zappia, V. The protective effect of the olive oil polyphenol (3,4-dihydroxyphenyl)ethanol counteracts reactive oxygen metabolite-induced cytotoxicity in Caco-2 cells. *J. Nutr.* **1997**, *127*, 286−292.

(32) Liu, L.-N.; Mei, Q.-B.; Liu, L.; Zhang, F.; Liu, Z.-G.; Wang, Z.-P.; Wang, R.-T. Protective effects of *Rheum tanguticum* polysaccharide against hydrogen peroxide-induced intestinal epithelial cell injury. *World J. Gastroenterol.* **2005**, *11*, 1503−1507.

(33) Ross, G. M.; McMillan, T. J.; Wilcox, P.; Collins, A. R. The single cell microgel electrophoresis assay (comet assay): technical aspects and applications. Report on the 5th LH Gray Trust Workshop, Institute of Cancer Research, 1994. *Mutat. Res.* **1995**, *337*, 57−60.

(34) Collins, A.; Dusinska, M.; Franklin, M.; Somorovska, M.; Petrovska, H.; Duthie, S., Fillion, L.; Panayiotidis, M.; Raslova, K.; Vaughan, N. Comet assay in human biomonitoring studies: reliability, validation and applications. *Environ. Mol. Mutagen.* **1997**, *30*, 139−146.

(35) Gabelova, A.; Pleskova, M. Failure of carboxymethylglucan to inhibit oxidative DNA damage induced by hydroxyl radicals or singlet oxygen. *Neoplasma* **2000**, *47*, 354−361.

(36) Jackson, S. P. Sensing and repairing DNA double-strand breaks. *Carcinogenesis* **2002**, *23*, 687−696.

(37) Schildkraut, E.; Miller, C. A.; Nickoloff, J. A. Gene conversion and deletion on frequencies during double strand break repair in human cells are controlled by the distance between direct repeats. *Nucleic Acids Res.* **2005**, *33*, 1574−1580.

(38) Leedham, S. J.; Brittan, M.; McDonald, S. A. C.; Wright, N. A. Intestinal stem cells. *J. Cell. Mol. Med.* **2005**, *9*, 11−24.

(39) Radtke, F.; Clevers, H. Self-renewal and cancer of the gut: two sides of a coin. *Science* **2005**, *307*, 1904−1909.

(40) Marklund, S. L.; Westman, G.; Lundgren, E.; Roos, G. Copper- and zinc-containing superoxide dismutase, manganese-containing superoxide dismutase, catalase, and glutathione peroxidase in normal and neoplastic human cell lines and normal human tissues. *Cancer Res.* **1982**, *42*, 1955−1961.

(41) Grisham, M. B.; Macdermott, R. P.; Deitch, E. A. Oxidant defense mechanisms in the human colon. *Inflammation* **1990**, *14*, 669−680.

(42) Schonbaum, G. R.; Chance, B. Catalase. In *The Enzymes*, 2nd ed.; Boyer, P. D., Ed.; New York Academy, 1976; Vol. XIII, pp 363−408.

(43) Ogura, Y. Catalase activity at high concentration of hydrogen peroxide. *Arch. Biochem. Biophys.* **1955**, *57*, 288−300.

(44) Fridovich, I. Superoxide anion radical, superoxide dismutases and related matters. *J. Biol. Chem.* **1997**, *272*, 18515−18517.

(45) Reische, D. W.; Lillard, D. A.; Eitenmiller, R. R. Antioxidants. In *Food Lipids*; Akoh, C. C., Min, D. B., Eds.; Dekker: New York, 1998; pp 423−422.

(46) Chaudiere, J.; Ferrari-Iliou, R. Intracellular antioxidants: from chemical to biochemical mechanisms. *Food Chem. Toxicol.* **1999**, *37*, 949−962.

(47) Nicholls, P. Contribution of catalase and glutathione peroxidase to red cell peroxide removal. *Biochim. Biophys. Acta* **1972**, *279*, 306−309.

(48) Bray, R. C.; Cockle, S. A.; Fielden, E. M.; Roberts, P. B.; Rotilio, G.; Calabrese, L. Reduction and inactivation of superoxide dismutase by hydrogen peroxide. *Biochem. J.* **1974**, *139*, 43−48.

(49) Symonyan, M. A.; Nalbandyan, R. M. Interaction of hydrogen peroxide with superoxide dismutase from erythrocytes. *FEBS Lett*. **1972**, *28*, 22−24.
(50) Jhonson, M. A.; Macdonald, T. L. Accelerated CuZn−SOD-mediated oxidation and reduction in the presence of hydrogen peroxide. *Biochem. Biophys. Res. Commun*. **2004**, *324*, 446−450.
(51) Blum, J.; Fridovich, I. Inactivation of glutathione peroxidase by superoxide radical. *Arch. Biochem. Biophys*. **1985**, *240*, 500−508.
(52) Sinet, P. M.; Garber, P. Inactivation of the human copper−zinc superoxide dismutase during exposure to the superoxide radical and hydrogen peroxide. *Arch. Biochem. Biophys*. **1981**, *212*, 411−416.

Received for review May 24, 2005. Revised manuscript received August 29, 2005. Accepted September 1, 2005.

JF0512003